The energy transfer model of nonphotochemical quenching: lessons from the minor CP29 antenna complex of plants

Margherita Lapillo, Edoardo Cignoni, Lorenzo Cupellini*, Benedetta Mennucci*

Dipartimento di Chimica e Chimica Industriale, Università di Pisa, Via G. Moruzzi 13, 56124 Pisa, Italy

Abstract

Antenna complexes in photosystems of plants and green algae are able to switch between a light-harvesting unquenched conformation and a quenched conformation so to avoid photodamage. When the switch is activated, nonphotochemical quenching (NPQ) mechanisms take place for an efficient deactivation of excess excitation energy. The molecular details of these mechanisms have not been fully clarified but different hypotheses have been proposed. Among them, a popular one involves excitation energy transfer (EET) from the singlet excited Chls to the lowest singlet state (S_1) of carotenoids. In this work, we combine such model with μs-long molecular dynamics simulations of the CP29 minor antenna complex to investigate how conformational fluctuations affect the electronic couplings and the final EET quenching. The computational framework is applied to both CP29 embedding violaxanthin and zeaxantin in its L2 site. Our results demonstrate that the EET model is rather insensitive to physically reasonable variations in single chlorophyll-carotenoid couplings, and that very large conformational changes would be needed to see the large variation of the complex lifetime expected in the switch from light-harvesting to quenched state. We show, however, that a major role in regulating the EET quenching is played by the S_1 energy of the carotenoid, in line with very recent spectroscopy experiments.

1. Introduction

In the thylakoid membrane of plants and green algae, pigment-protein antenna complexes are used for maximizing the energy supply to reaction centers under limiting light, but in excess light conditions their excitation can go beyond the capacity of reaction centers of accepting and transforming the associated energy [1]. If this happens, singlet-excited states of Chl undergo intersystem crossing into triplets, which react with molecular oxygen and ultimately result in photodamage. To avoid this cascade of events, Photosystem II (PSII) uses different mechanisms of regulation of its quantum efficiency, which are collectively referred to as non-photochemical quenching (NPQ) [2–6]. Thanks to these mechanisms, most of the absorbed photons are dissipated as harmless heat. The major component of NPQ, energy-dependent quenching (qE), is rapidly reversible, and is triggered by a proton gradient across the thylakoid membrane [4, 5].

Although NPQ is nowadays a well-established concept in photoregulation of many photosynthetic organisms, a complete identification of the exact molecular mechanisms is still missing. What seems more realistic is that there is not a unique mechanism but different strategies that the various types of antenna complexes have optimized [5–8]. Both the major LHCII antenna of PSII and the minor antennas, in particular CP29, have been shown to participate in NPQ [9–12]. Several experimental lines of evidence indicate that the antenna proteins change conformation to switch between the light-harvesting and the quenching functional state [13–17]. This conformational change is mediated, *in vivo*, by a non-pigment-binding pH sensor protein, the photosystem II subunit S (PsbS) [18–20], which senses the lumen acidification caused by excess irradiation. Also in this case, however, there are not definitive answers about the type of conformational change and the molecular quenching processes activated by such a change. One of the commonly suggested hypothesis for the quenching reaction is the energy transfer (EET) from the singlet excited Chls to the lowest singlet state (S_1) of carotenoids (Cars) [4, 21]. However, fast electron transfers from the carotenoid to the excited chlorophyll, followed by charge recombination in the ground state, cannot be excluded [3, 10, 22]. Finally, Chl-Chl charge-transfer states and Chl-Car exciton states have also been proposed as quenching intermediates [23, 24].

The main reason for the large uncertainty on both the quenching processes and the molecular mechanisms is the difficulty of directly observing and quantifying the single energy or charge-transfer process within the complex. Spectroscopic techniques such as transient absorption, two-dimensional electronic spectroscopy, and time-resolved fluorescence give crucial and quantitative insight into the quenching process, especially when combined with site-directed mutagenesis. However, due to the complex-

*Corresponding author

Email addresses: lorenzo.cupellini@unipi.it (Lorenzo Cupellini), benedetta.mennucci@unipi.it (Benedetta Mennucci)

ity of the system, even these techniques cannot unequivocally disentangle the elementary kinetic steps and assign the signals to individual pigments. These experiments can however measure the lifetime of the complex in both quenched and unquenched complexes: combining these measurements with reliable molecular models could represent an extremely powerful tool to discharge or confirm the different quenching processes proposed so far. However, building such a reliable model is extremely challenging even for an isolated complex and selecting "a priori" a specific mechanism. In fact, single-pigment properties and inter-pigment couplings would be needed for all the Chls and Cars, and thier calculation would require to properly include the dynamic effects of the protein and the external environment (membrane and solvent).

Due to this large complexity, the attempts appeared so far in the literature to simulate qE processes have used simplified approaches, which necessarily make assumptions not only on the type of quenching mechanism but also on the number and type of involved pigments. Moreover, instead of explicitly calculating all the needed properties for the system of interest, they introduce parameters, either estimated from some experiments or obtained from modelistic systems, and commonly assume a static representation of the system through a single structure, generally the one determined by X-ray crystallography.

The first kinetic EET quenching model of LHCII included only luteins [25]. Then an all-pigment model was devised to include other carotenoids [26]. These models showed that the short fluorescence lifetime of the LHCII crystals [13] can be explained by relatively slow EET from the Q_y state of Chl a to the S_1 state of carotenoids. A newer model was developed with a more realistic spectral density for carotenoids (obtained by fitting the two-photon spectrum of Lut), and some QM optimization of the pigment geometries [27]. The same method was finally applied to CP29 [28]. Other models (for LHCII) instead used molecular dynamics (MD) simulations prior to coupling estimation but considered only luteins [29] or only the lutein in site L1 [30].

Here we focus our attention on the minor CP29 antenna complex of plants. CP29 shares many similarities with the LHCII monomer in terms of apoprotein structure and pigment binding sites [31–33]. Among the 13 Chl binding sites, 9 are occupied by Chl a, and 4 by Chl b (Figure 1b). More recently, a further Chl a (a616) was found between CP29 and the PSII core in the Cryo-EM structure of the PSII supercomplex [33]. In addition, CP29 binds three different carotenoids, *i.e.* a lutein in the L1 site, a violaxanthin (Vio), possibly substituted by a zeaxanthin (Zea), in the L2 site, and a neoxanthin (Neo) in the N1 site (Figure 1c). The particular carotenoid composition of CP29 helps us disentangle the effect of each carotenoid binding site on the quenching mechanism, and allows us to explore the role of the two different carotenoids in the L2 site. In fact, the xanthophyll cycle, where violaxanthin is reversibly de-epoxidized to zeaxanthin (Zea), was shown to be related to NPQ [5, 34–36]. In minor antenna complexes, Zea was proposed to participate in the quenching process [10, 12, 22]. While the substitution of Vio by Zea in the L2 site does not seem to occur *in vivo* [37], CP29 containing Zea was isolated from mutant plants which accumulate Zea constitutively [38].

Calculating Chl-Car couplings along microsecond molecular dynamics (MD) trajectories of CP29 containing Vio or Zea, we show that the EET quenching model predicts a fluorescence lifetime that is rather insensitive to the variations in the relative position/orientations of the pigments, challenging the model of a conformation-modulated coupling switch. However, we show that an important role in the tuning of the EET mechanism can be played by the energy of the Car S_1 state which, in turn, can be regulated by protein-induced geometrical distortions.

The paper is organized as follows: in Section 2 we outline the MD strategy and the all-pigment EET model. In Section 3.1 we analyze the microsecond MD trajectories of CP29 embedding Vio or Zea. Then we discuss the results obtained using the all-pigment model (3.2), a model containing only Lutein (3.3), and the model containing Zea in the L2 site (3.4). Finally, we discuss our findings in Section 4 in relation to the most recent experimental and modellistic results on LHCII and CP29.

2. Methods

2.1. Molecular dynamics

We performed four independent 3 μs classical molecular dynamics simulations (MDs) of CP29 embedded in a model membrane. All simulations were run by using the Cryo-EM structure of CP29 solved in 2016 by Wei et al. (PDB code 3JCU, Chain R, 3.2 Å resolution) as starting structure [33]. Two MDs were run for CP29 containing violaxanthin in the L2 site (CP29-Vio), and two additional MDs were run for CP29 containing zeaxanthin (CP29-Zea). The CP29 structure was embedded into a pre-equilibrated DOPC membrane, solvated with ∼25 300 water molecules, with a 0.15 M KCl concentration (See details in the Supplementary Information). The structures were minimized and equilibrated at 300 K with a protocol similar to previous simulations of CP29 and LHCII [29, 39] and of the entire PSII [40]. The MDs were run with a timestep of 2 fs and saved every 100 ps for the analysis, for a total of 30 000 frames per simulation. The Amber ff14SB [41] and lipid14 [42] force fields were used for protein and lipids, respectively, whereas pigments were described with ad-hoc parameters [43, 44]. All simulations were run with Amber 18 [45], and analyzed with the CPPTRAJ program [46] and its python interface pytraj.

More details about the four MD simulations are reported in the Supplementary Information.

2.2. The all-pigment EET Model

In our analysis, we use the same kinetic model established in Ref. 28 for the X-ray structure of CP29 [31],

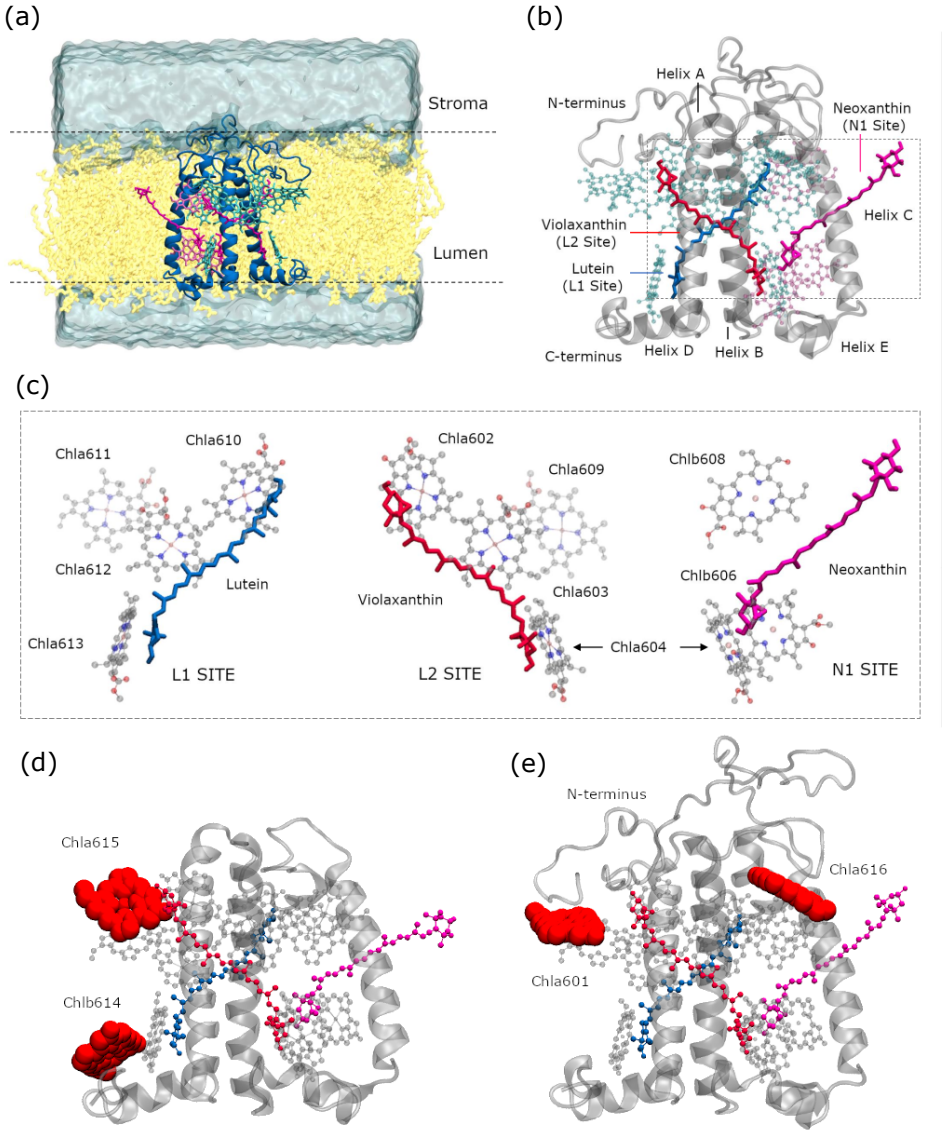

Figure 1: Molecular structure of the CP29 monomer. (a) Longitudinal section of the simulation system. The CP29 complex was embedded into a water solvateted bylaier DOPC membrane (lipids in yellow and water in glass cyan). The CP29 complex orientation inside the mambrane is highlited in the image. (b) Side-view of the CP29-complex showing the five protein structural domains, the positions of the three carotenoids and the chlorophyll network (ten Chl a colored in cyan and three Chl b in mauve). (c) Enlarged view of the significant Chl-Car interaction domains within the CP29 complex, namely L1, L2 and N1 sites. (d)-(e) Structural differences between (d) the CP29 X-ray structure [31] and (e) the recently resolved Cryo-EM structure [33]. In the latter, Chl b614 is missing while Chl a615 corresponds with a slightly differently oriented Chl a601. Moreover, Chl a616 and the whole N-terminus has been solved. Chlorophylls are depicted in red Van der Waals spheres for clarity.

but we generalize it to different μs-long MD simulations of CP29 in the membrane, starting from the Cryo-EM structure from spinach (3JCU) [33]. This model, along with the previous ones on LHCII [26, 27], is an "all-pigment" model, because it takes into account all the chlorophylls and all the carotenoids in the complex.

It should be noted that the X-ray CP29 structure lacks the entire N-terminus, which is instead entirely solved in the Cryo-EM structure [33]. In addition, there are some differences in the pigment composition of the two structures, which are summarized in Figure 1(d,e). The Cryo-EM structure presents a new Chl, a616, which is bound at the interface between CP29 and the PSII core [33], and is likely lost during purification and isolation of CP29 [47]; for this reason, we excluded Chl a616 from our model. Moreover, Chl a615 (as assigned in the X-ray structure [31]) has a different position in the Cryo-EM structure, and was reassigned to Chl a601. This difference in position was confirmed in the pea Cryo-EM structure and explained by the disruption of the N-terminus in the X-ray CP29 structure [48]. Finally, Chl b614 is missing in the Cryo-EM structure. In our model we decided to disregard Chl b614, which, being a Chl b (i.e. a high energy site), should not affect the quenching dynamics significantly. We keep the chlorophyll numbering of Ref 28 for clarity.

In the kinetic model, EET between all pigments of the complex is assumed to be an incoherent hopping between the various pigments. However, there are a few strongly coupled pigment clusters in which the excitation is considered delocalized. For CP29, these clusters are *a610-a611-a612*, *a602-a615*, and *a603-a609* [28]. The EET dynamics is modeled with the following kinetic model (Pauli master equation) [28]:

$$\frac{\mathrm{d}}{\mathrm{d}t}P_n = \sum_{m\neq n}\Big[k_{m\to n}P_m(t) - k_{n\to m}P_n(t)\Big] \qquad (1)$$

where m/n is either a site, an exciton state in one of the clusters, or the ground state. The rates $k_{\mathrm{GS}\to n}$ are assumed to be zero, *i.e.* dissipation to the ground state is irreversible. Each pigment can decay to the ground state with a rate that corresponds to a 4 ns lifetime for the Chls and a 10 ps lifetime for the Cars. In all calculations, we assume the initial population to be equally distributed on all the chlorophylls.

In order to determine the rates, we build the exciton Hamiltonian matrix of CP29. Its diagonal entries are the site energies of the pigments $\mathcal{E}_i$, and the off-diagonal entries are the exciton couplings V_{ij}. Within the partially delocalized scheme described above, the Hamiltonian matrix is diagonalized only within the three pigment clusters. The Hamiltonian is block-transformed to diagonalize these clusters. The EET rates $k_{n\to m}$ depend on the couplings and site energies as detailed below, the only exceptions being the rates within clusters. The downhill rates within these clusters are set to 10 ps^{-1} (*i.e.* instantaneous), while the uphill rates depend on the Boltzmann factor.

More details about the kinetic model are reported in the Supplementary Information.

2.3. Inter-site rates

The rates between sites/clusters are computed in the Förster weak coupling limit:

$$k_{m\to n} = \frac{2\pi}{\hbar}\,|V_{mn}|^2\,J_{mn} \qquad (2)$$

where V_{mn} is the EET coupling, and the spectral overlap J_{nm} is computed as

$$J_{mn} = \frac{1}{\pi}\,\Re\int_0^\infty \exp\left\{-i\omega_{nm}t - 2i\lambda_m t - g_n(t) - g_m(t)\right\}\mathrm{d}t \qquad (3)$$

The lineshape functions $g(t)$ are obtained directly from the corresponding spectral densities. We used exactly the same spectral densities as in Ref. 28, namely, the B777 spectral density of Renger and Marcus [49] was used for the Chls, whereas the spectral density obtained by Fox et al. [27] by fitting the two-photon excitation spectrum of Lut [50] was used for Cars. For rates between localized sites and (Chl) excitonic states in the clusters, the spectral densities of the excitonic states are assumed identical to those of the sites, but the energies and couplings are not. Energies are obtained as the eigenvalues of the cluster Hamiltonian, and couplings are transformed accordingly.

2.4. Site energies and couplings

In this work, we used the same site energies as the earlier model [28], where the Chl site energies calculated by Müh et al. [51] were employed. The site energies for the S_1 state of carotenoids Lut, Vio, and Neo were taken from Ref. 28. The site energy for Zea was determined by considering that, in experiments, the S_1 state of Zea is $\sim$500 cm^{-1} below that of Vio [52].

The couplings among chlorophylls were taken from Ref. 51 and kept constant for the configurations generated by the various MD trajectories, in order to reproduce exactly the same inter-Chl dynamics as in Ref. 28, where those Chl-Chl couplings were used. In any case, we assessed the role of inter-Chl coupling fluctuations (see the Supplementary Information) and found that, when using the results of our MD simulations, they have negligible impact on the lifetime of the complex. The couplings between chlorophylls and the S_1 states of carotenoids were instead calculated for each configuration as the interaction between transition charges (TrEsp [53]) of the two interacting pigments. The transition charges for the Q_y state of Chls were computed at the TDDFT B3LYP/6-31+G(d) level of theory; those for the S_1 state of Cars were obtained at the DFT-MRCI level of theory [54]. Car-Chl couplings were calculated on the Cryo-EM structure and along the MD trajectories.

The couplings obtained at the DFT-MRCI level were significantly larger than the ones calculated by Fox et al. [28] (See Table S1), while the magnitude of the

Lut/a612 coupling is more similar to the one calculated with the TrEsp RASSCF charges [55]. These differences find an explanation in the difficulty of QM methods in accurately describing the S1 state. It is in fact important to note that S1 is characterized by a strong double-excitation character, with a small mixing to singly excited configurations. In a pure double excitation the transition density would be identically null, and it is the small mixing that allows a non-zero S0-S1 transition density. Because the magnitude of the transition charges is proportional to this mixing, it is evident that they can vary significantly between different QM methods.

Here, with the aim of keeping our model consistent with Ref. 28, we scaled the DFT-MRCI transition charges by a factor 3.7, so that our largest Lut-Chl and Lut-Vio couplings are of the same magnitude as the largest coupling of Ref. 28. The RASSCF charges of Ref. 55 were scaled in order to reach the same value for the largest Lut-Chl coupling, and used to compare our results in the Lutein-only EET model.

3. Results

As described in the Introduction, it is now widely accepted that antenna complexes undergo a conformational change to switch their function from light-harvesting to quenching. This switch can be experimentally evidenced though measurements of change in the excited-state lifetime of the complex. For monomeric CP29, lifetimes changing from ∼100 ps to about 4 ns have been recently observed [56], and associated to quenched and light-harvesting states, respectively.

As described in the Methods, our MD simulations were run by using as starting structure the Cryo-EM structure of CP29 [33]. For model building this structure, the X-ray structure of CP29 was fitted into the Cryo-EM map. As such, the resulting arrangement of the pigments inside the protein matrix resembles the one from X-ray which is known to correspond to a quenched state with a lifetime of ∼150 ps [28]. We can therefore conclude that our initial structure is a quenched state as well.

3.1. Structural fluctuations from MD trajectories of CP29-Vio and CP29-Zea

In order to understand the impact of conformational fluctuations on the Chl-Car couplings, and then on the extent of quenching, we ran two replicas of a 3 μs MD simulation of CP29-Vio, starting from the Cryo-EM structure. In addition, to evaluate the effect of the substitution of Vio with Zea in the L2 site, we performed two additional 3 μs MD simulations of CP29-Zea. In all MDs, the CP29 complex has been simulated within a double layer membrane model (Figure 1a). We will refer to these simulations as MD-Vio 1, MD-Vio 2, MD-Zea 1 and MD-Zea 2, for simplicity.

Before analyzing the specific EET L1 and L2 sites, we analyzed the extended N-terminus loop, which was not resolved in the earlier CP29 structure by Pan et al.[31]. The CP29 loop is ∼50 amino acid residues long and, in the Cryo-EM structure of the entire PSII, is completely extended and has the function to bind the neighboring CP47 [33, 48]. In all of our MD simulations, the N-terminus undergoes a wide displacement from its starting conformation (Figure S2), with RMSD values (computed with the CryoEM structure as reference) reaching values as high as 16 Å. This result is in agreement with EPR studies performed on the solubilized CP29 complex [57], suggesting the N-terminus is a highly flexible and highly disordered domain, which may adopt several different conformations in isolated CP29.

Moving now to the pigments in sites L1 and L2, Figure 2a-c show that they present a relatively low mobility, and remain stable around their initial positions (See also Figures S4 and S5). In all MDs, we observed that Car-Chl mutual distances undergo just slight changes when compared to the initial Cryo-EM structure, and the respective fluctuations are around ∼1 Å. To further investigate the motion of the chromophores, we evaluated xanthophylls orientation by computing the angle between their backbone and the z-axis (Figure 2d) [58]. For Lutein in site L1, the angle remains constant around ∼67° suggesting that Lutein motion is strongly limited within the complex. Both xanthophylls in site L2 have a similar stability to Lut in L1; however, the conversion of Vio into Zea leads to a slight decrease in the carotenoid mobility, as shown by the limited orientations assumed by Zea when compared with Vio (Figure 2d). The time evolution of the computed angles, indeed, shows a more variable trend for Vio than for Zea, mostly in the first half of both simulations. Contrary to the Cars in the L1/L2 sites, Neo, which is peripherally bound at the N1 site, experiences wide deviations from its initial position, with one end bending outside the complex and interacting with the membrane lipids, while the other one is strongly anchored to the protein backbone.

The observed difference in Vio/Zea mobility might influence the distances and mutual orientations of the Car-Chl pairs, which are important for tuning the respective electronic couplings, as previously shown by Balevičius et al. for LHCII [29], and also seen for the couplings with the Car S_2 state [58, 59]. We thus computed the angles φ_{yx} and φ_{zx} that determine the orientation of the Car backbone relative to the ring of the middle-cofacial Chl, that is, a612 for site L1 and a603 for site L2. The distribution of these angles is reported in Figure 2e for sites L1 (Lut-a612 pair) and L2 (Vio/Zea-a603 pair, See Figure 2e for angle definitions). The results obtained in the present trajectories are in line with those of LHCII [29] in terms of fluctuation in the relative pigments orientation, even if some differences are present. In site L1, the φ_{yx} angle is higher than in LHCII, while the φ_{zx} angle is lower, meaning probably that in CP29 the Car-Chl pairs have an overall more parallel arrangement than in the LHCII

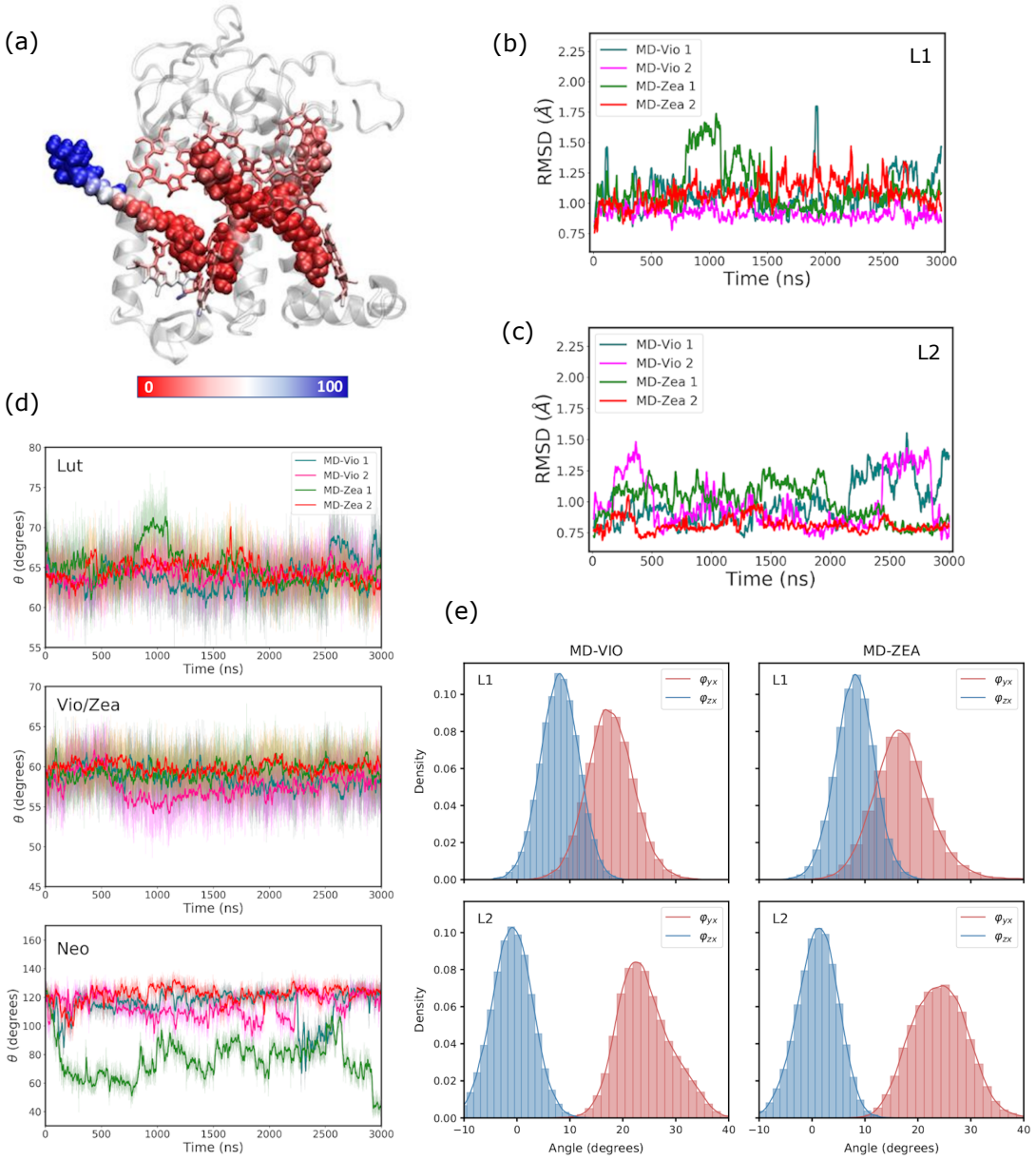

Figure 2: Molecular dynamics of the CP29 monomer. (a) Focus on L1, L2 and N1 domains as from MD simulations colored according to their B-factor values (from red to blue, 0-100 A^2). (b, c) RMSD computed for pigments in the L1 and L2 sites. The moving average of the RMSD is shown for a clearer visualization. The two sites have been aligned to the corresponding site in the reference structure (3JCU) before computing the RMSD. (d) Xanthopylls orientations computed along the four MDs. The orientation has been determined as the angle between a vector directed along the linear chain of the carotenoid and the z axis. (e) Distribution of φ_{yx} and φ_{zx} angles for L1 and L2 sites along MD replicas. In detail, φ_{yx} angle corresponds to the projection of the carotenoid backbone axis (C_9-C_{30} axis) in the xy plane, whereas, φ_{zx} angle corresponds to the projection of the backbone axis in the xz plane. Distributions are shown in red (φ_{yx} angle) and blu (φ_{yx} angle), respectively.

monomer. However, the fluctuations of both angles have the same extent as in LHCII. The differences are more pronounced in site L2, which here contains Vio/Zea, whereas it contains Lut in LHCII. In CP29 larger fluctuations are found in the Vio/a603 orientation, and the distribution of angles is more skewed (Figure 2e). The substitution of Vio with Zea moves the φ_{yx} rotation angle to higher values.

The substitution of Vio with Zea also affects the mobility of the pigments cluster in L2 site. Considering the hypothesis that Zea may have a role as an allosteric modulator [4, 5, 60, 61], we evaluated the effect of its insertion on the Car-Chls mutual orientation in L1 site, by comparing pigments fluctuations in the L1 site between trajectories containing Vio or Zea in the L2 site. Figure 2b, c shows pigments fluctuation as the average RMSD of the main Car-Chls pairs in sites L1 and L2 computed for all the simulations with respect to the initial Cryo-EM structure. We find no clear effect of Zea substitution on the dynamics of Lutein in L1, since all MD trajectories showed similar fluctuations of the pigments cluster. Considering the above points, therefore, the presence of Zea in L2 seems not to affect at all pigments position in L1 site.

Xanthophyll mobility was further assessed in terms of fluctuantions of their dihedral angles along the different MDs. In fact, it was suggested that the dihedral conformation of xanthophylls can tune their light-harvesting or photoprotective function [62]. We therefore evaluated the time evolution of the two dihedral angles associated to the two end-rings of the xanthophylls in sites L1 and L2 along all the MDs (Figures S7 and S8, respectively). For Lutein in L1, we observed a higher mobility of the dihedral angles which switch alternately from *trans* to *cis* conformations, thus causing the rotation of the Lut end-ring at the lumenal side. In line with previous studies [62], we find that different Lut configurations are possible within the L1 site and dihedral switches are favoured mostly on the lumenal side of the complex. On the other hand, the dihedrals of both Vio and Zea in L2 site show less conformational variability than Lut. We can again notice a lower mobility for Zea, which never changes dihedral conformation.

3.2. All-pigment EET model

As a preliminary test, we applied the quenching model to the Cryo-EM structure. The Chl-Car coupling values are generally similar to those reported in Ref. [28], except for couplings involving Neo, which in our calculations are significantly smaller. The full comparison is reported in Figure S1, showing that the main differences are due to the method used for the calculations, rather than the different structure. Nonetheless, our model predicts a lifetime (174 ps) for the Cryo-EM structure that is in very close agreement with the one reported in Ref. [28].

We then computed the Chl-Car EET couplings averaged over ∼60 000 configurations extracted from the two replicas of the MD trajectory of CP29 containing Vio. The couplings remain generally close to the values computed for the Cryo-EM structure, the only exceptions being the coupling of Vio with a602 and a603, and of Lut with a611 and a613. In addition, couplings for the two trajectories agree well with one another, suggesting that the coupling averages are well converged (see Table S2). The lifetimes of the complex computed with these parameters are reported in Table 1 where they are compared with that obtained for the Cryo-EM structure.

Table 1: Summary of CP29 lifetimes (ps) and quenching quantum yields (QY, %) computed on the Cryo-EM structure, on the four MD replicas and for clusters resulting from the cluster analysis performed on couplings along MDs-Vio. MD-based lifetimes were computed from the average couplings of each MD.

System	Lifetime (ps)	QY (%)		
		Lut	Vio/Zea	Neo
Cryo-EM	174	51	43	2
MD-Vio 1	195	64	30	1
MD-Vio 2	197	66	28	1
MD-Zea 1	162	52	44	0
MD-Zea 2	149	49	47	1
Cluster 1	193	65	29	1
Cluster 2	182	60	35	1
Cluster 3	209	69	25	1
Cluster 4	230	76	18	1

Overall, the EET model predicts a very small difference, both in complex lifetime and in the relative quantum yield of quenching, between the Cryo-EM structure and the average on the MD trajectories.

In addition to the average results, MD data give access to coupling variability arising from both fast and slow structural fluctuations. While fast fluctuations do not influence the measured lifetime of the complex, because the EET rates are averaged over the fluorescence lifetime, slow fluctuations indicate the presence of distinct conformations with possibly different EET rates. With the aim of understanding the origin of the variability of couplings, while reducing as much as possible the effect of fast fluctuations, we performed a k-means clustering (see details in the Supplementary Information) of all the Car-Chl coupling values, joining the couplings of the two MD-Vio replicas. This gives an estimate of how the conformations of the complex differ in quenching level.

Figure 3 shows some of the average Car-Chl couplings calculated for the different clusters (we show the pairs with the largest couplings in sites L1 and L2). The results show a larger variability of the couplings involving Vio with respect to the ones involving Lut. We finally computed the lifetime of the complex using the Car-Chl couplings for each cluster. The results are reported in Table 1, along with the lifetime computed along the whole MDs. While the clusters show a difference in lifetime, this difference is quite small, and is not compatible with a switch between the quenched and the light-harvesting state. The maximum lifetime (Cluster 4) is in fact only ∼24% larger than the lifetime calculated on the Cryo-EM structure.

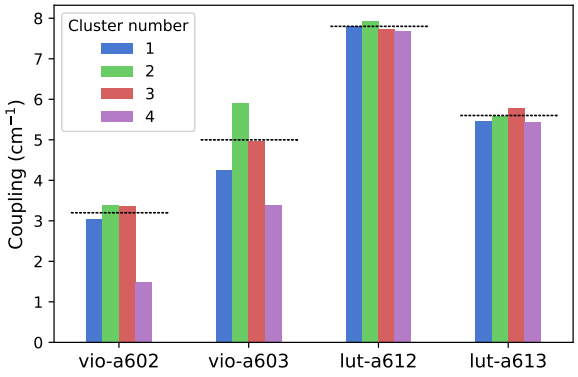

Figure 3: Cluster analysis of Car-Chl EET couplings along the two MD replicas of CP29-Vio, namely MD-Vio 1 and MD-Vio 2. Only the Car-Chl pairs with the largest couplings in sites L1 and L2 are shown. For each Car-Chl pair, the average coupling over the two MDs is shown as a horizontal black dashed line (exact average values are provided in Table S2). The optimal number of clusters was determined by silhouette analysis (see details in the Supplementary Information).

We note that the largest L1 coupling, between Lut and Chl a612, shows a remarkably low variability among clusters. As shown in Figure S11, the distribution of the Lut-a612 coupling is very narrow compared with the corresponding largest coupling in L2 (Vio-a603). The relative standard deviation of the Lut-a612 coupling is ∼30%, in comparison to the ∼80% of the Vio-a603 coupling (Table S2). This finding is in stark contrast with the results of Balevičius *et al.* [29] for LHCII, where the Lut-a612 coupling showed considerable variations (from ∼ 0 to 8 cm^{-1}). This marked difference cannot be ascribed to the different fluctuations in Lut/a612 orientations, which are very similar in the present MD trajectories and in the LHCII trajectory (See above). Instead, the discrepancy likely arises from the different orientation dependence of the couplings calculated in Ref. 29 with a semiempirical method (AM1-CAS-CI) compared with the method used in this work. Notably, the couplings calculated with several *ab initio* methods also show a different orientation dependence with respect to the semiempirical method [55].

The analysis performed on the MD has shown that, within the current EET quenching model, the fluctuations in the positions of the pigments are not sufficient to turn off the quenching and switch to the light-harvesting state. On the other hand, Daskalakis *et al.* have shown with enhanced sampling MD that a rearrangement of the Lut-a612 pair in site L1 could have a significant influence on the lifetime of the LHCII complex [30], although their analysis neglects all the other Car-Chl pairs. It would be therefore interesting to know whether a substantial change in the relative position of one Car-Chl pair would be sufficient to increase the lifetime of the complex to the levels observed in unquenched CP29.

Taking this reasoning to the limit, we assume that a given conformational change can reduce one Chl-Car coupling to zero, and we compute the effect of this change on the excited-state lifetime of CP29. Figure 4 shows how the CP29 lifetime increases when single Car-Chl couplings either in the L1 site or in the L2 site are set to zero. From these results it is clear that, when one of the Chl-Car couplings is set to zero, the energy is still efficiently quenched through one of the other Chl-Car connections. As a result, the lifetime of the complex increases only slightly. For example, removing the Lut-a612 coupling increases the lifetime by only ∼25%. Moreover, removing all the couplings in the L1 site (e.g. fully inactivating L1 as a possible quenching site) increases the lifetime only to 0.5 ns, which is still significantly shorter than the lifetime of unquenched CP29.

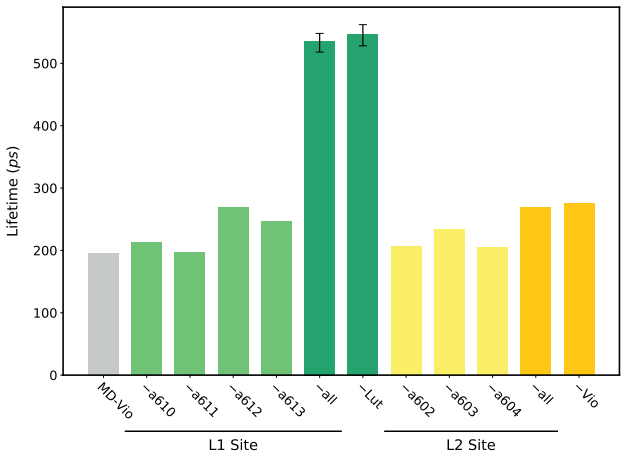

Figure 4: Excited-state lifetime of CP29 obtained by removing some of the couplings in the all-pigments model. Labels on the x-axis denote the couplings that have been set to zero. " - Lut" and " - Vio" denote kinetic models obtained by removing completely Lut or Vio. The analysis was performed on the data coming from both MD replicas (MD-Vio 1 and MD-VIo 2). Error bars representing the difference between replicas are shown as black lines. Only those corresponding to the largest calculated errors are non-negligible and shown in the plot.

3.3. Lutein model

Due to the dark character of the Car S_1 state [52, 63], the precise value of its excitation energy is not known. Here, we change the previous model by assuming that the site energy of Vio is too high for it to be resonant with the surrounding chlorophylls. As such, all the Chl → Vio EET transfers may be neglected under this assumption. We may further simplify the model considering that Lut is only sensibly coupled with chlorophylls in the L1 site.

Within this framework, Lut is most strongly coupled with a612, which faces the middle of the Lut backbone (Figure 1c). However, the relative magnitude of the couplings depend on the QM method used. With the DFT-MRCI TrEsp charges, the couplings with a610 and a613 are only slightly smaller (see Table S1). On the other hand, using the RASSCF charges [55], the coupling with

a612 is much larger than the others. Using the two sets of charges, we can predict a different effect of removing the various Chls from the L1 site (Figure S12). Moreover, we have considered a further simplified model which neglects all the couplings except for Lut-a612. This leaves us with a minimal "Only a612" model, which has been the basis of several works aimed at understanding the relationship between conformation and quenching in LHCII [29, 30, 64].

The two Lutein models have been further used to assess the influence of Lut site energy on the lifetime of the complex. The site energy of Lut has been varied in the interval $[10\,000, 20\,000]$ cm^{-1}, computing the lifetime for 50 equally spaced values in this interval. The influence of the Lut-a612 coupling has also been investigated. For each value of the site energy, the lifetime has been computed also for a small (2.9 cm^{-1}) and a large coupling (11.6 cm^{-1}), corresponding to the Lut-a612 coupling averaged over the MD trajectory plus or minus two standard deviations, respectively (see Table S2).

The complex lifetime and its variability are shown in Figure 5 for the minimal (Only-a612) and the full Lutein-model. The impact of both the coupling and the S_1 energy on the lifetime of CP29 is further shown in Figure S8.

If we use the Only-a612 model (Figure 5a), we obtain a large range of Lutein S_1 energies (approximately $[14\,000, 17\,000]$ cm^{-1}) in which the lifetime is approximately constant around an average value of ∼450 ps, and a small range (around $[17\,000, 18\,000]$ cm^{-1}) where the complex rapidly switches from a quenched to an unquenched state (lifetime of ∼4 ns). We also note that a reduction of about 5 cm^{-1} of the Lut-a612 coupling is needed to significantly increase the lifetime of the complex to ∼2 ns, compatible with an unquenched state of CP29 (Figure S8a). As explained above, while in our MD trajectories we do observe variations in some of the couplings, the Lut-a612 coupling remains quite large throughout the MDs.

When we move to "full Lutein model" (Figure 5b and S8b) we see that, besides shifting the curve towards smaller lifetimes, addition of the other Chls softens the impact of Lut/a612 coupling variations on the complex lifetime. On the contrary, the sensitivity to the S_1 energy variation clearly remains unchanged.

From these results, it is quite clear that a significant variation in couplings or S_1 energy is needed for the unquenched lifetime to be recovered. In particular, the coupling reduction needed for switching off the quenching cannot be achieved with a small change in the relative positions of Lut and Chl a612. In addition, the presence of other chlorophylls requires a reduction of all the Lut-Chl couplings to turn off the quenching. On the other hand, raising the site energy of Lut above ∼17 500 cm^{-1} seems to be sufficient to cause a sharp increase in the complex lifetime; however, this would mean that the S_1 energy of Lut has to increase by more than 2 000 cm^{-1}. It is important to recall that this large blue-shift is mainly determined by the value of the reorganization energy used for the S_1 state of Lut that here has been set to a quite large value, 2250 cm^{-1}. Such a value, in fact makes the the spectral overlap with Chl a emission weakly dependent on the S_1 energy. The value of the reorganization energy was obtained by fitting the two-photon excitation spectrum of Lut in octanol [50]. It is possible that, due to the constraints of the protein environment, the reorganization energy of Lut is smaller in CP29, thus making the spectral overlap and also the lifetime of the complex more sensitive to Lut S_1 energy.

3.4. The role of Zea

As a further analysis, we evaluate the effect of substituting violaxanthyn with zeaxanthin in the L2 site. We applied the EET quenching model to the two CP29-Zea MDs, computing Chl-Car couplings along ∼60 000 trajectory frames. The EET coupling values calculated for the most significant Zea-Chl pairs in the L2 site are reported in Figure 6a and compared with those previously computed for the MD trajectories containing Vio. The couplings differ slightly from those computed for Vio, showing an average increase of about 1 cm^{-1}. Moreover, the calculated average values among the two replicas are close to each other, suggesting again that the MDs are reasonably well equilibrated. An exception is given by the coupling of Zea with Chl a603, which is different in the two MDs owing to the different orientation of the Zea-a603 pair, as shown by the distribution of the φ_{yx} angle in Figure S9.

The lifetime in the presence of Zea was finally computed using a site energy of Zea 500 cm^{-1} lower than that of Vio [52] (see Table 1). The lifetimes calculated on the individual MDs reflect the Zea-a603 coupling variability, with ∼162 ps for the first replica and ∼149 ps for the second one. These lifetimes are slightly lower than the ones calculated on the Vio MD due the increase in Zea-Chl couplings and the lower site energy of Zea. If we use for Zea the same site energy as for Vio, we compute a lifetime of ∼182 ps, which is still lower than for CP29-Vio. These results suggest that a modest coupling variation is not able to substantially influence the complex lifetime.

To further investigate the role of Zea, we performed the same analysis reported above for Vio by setting one by one Chl-Car couplings to zero and computing the effect of this change on the complex lifetime. As shown in Figure 6b, the lifetime of the complex increases only slightly (∼10 to 25%) when one of the Chl-Car coupling of both L1 or L2 site was set to zero. Removing all the couplings in the L2(Zea) site has essentially the same effect observed in the MDs including Vio (Figure 4). On the contrary, removing all the couplings in the Lut-L1 site leads to a smaller increase of the lifetime for MDs containing Zea (only 0.29 ns), if compared to the increase obtained for Vio (0.5 ns). Without Lut, energy is still efficiently quenched through the main Chl-Zea channels. Unlike Vio, Zea seems to behave as a good EET energy acceptor from Chls, with an efficiency almost comparable to that of Lut.

Our calculations point to a direct role of Zea in the quenching, independent of the L1 site. It is important to

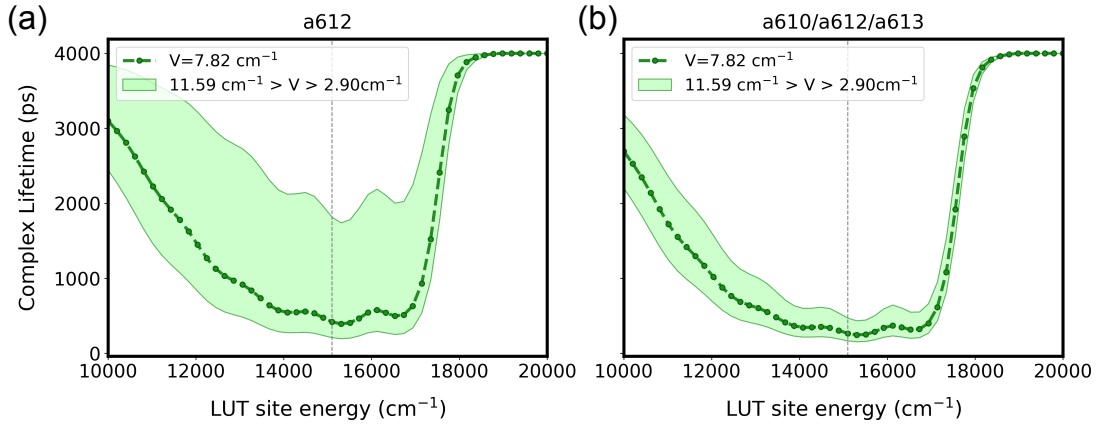

Figure 5: Complex lifetime vs Lut site energy in the two Lutein models: (a) Only-a612 and (b) Full L1 site. The dark green curve shows the variation of the lifetime when the average Lut/a612 coupling of the all-pigment model is used. The shaded region shows how the lifetime changes when varying the Lut/a612 coupling from V = 11.59 cm^{-1} to V = 2.90 cm^{-1}. The dashed vertical line indicates the site energy used in the all-pigment model.

note that the role of Zea in LHCII might be completely different, because LHCII contains Lut in the L2 site, and Vio/Zea in the V1 site at the interface between monomers of the trimer.[31, 32, 65] It was in fact shown that the fluorescence lifetime of LHCII is independent of Zea.[66] On the contrary, for CP29, there is evidence that Zea can restore quenching even in complexes lacking Chl a612.[67]

4. Discussion

The results presented so far allows us to try to make some conclusive remarks about different experimental/modellistic findings recently obtained either in CP29 or in LHCII. These are separately discussed here below

Site-directed mutagenesis experiments. The all-pigment models presented in the previous sections allow us to discuss the role of specific Car-Chl interactions in the context of the recent site-directed mutagenesis experiments in which some Chl are selectively removed from the complex. The most recent experiments on CP29 yield seemingly contrasting conclusions [56, 68]: Mascoli *et al.* [56] investigated the isolated CP29 and found that removing Chl a603 had no effect on the excited-state decay, whereas removing Chl a612 altered significantly the fastest decay component, implying that the main quenching site is L1. Guardini *et al.* [68] instead measured the NPQ activity of *in vivo* PSII with different mutations on CP29, which was not affected by Chl a612, but was significantly impaired by the lack of Chls a603 and a616. These *in vivo* results point to L2 as the main quenching site. Our all-pigment models predict a small effect of removing a single Car-Chl interaction, either in the L1 or in the L2 site. Nonetheless, from Figures 4 and 6b, we see that Chls a603 and a612 have the most important role in quenching within the respective sites. However, these two Chls have a similar effect, with no preference for either site.

The comparison with Ref. 68 is complicated by the fact that the *in vivo* NPQ activity in PSII might not be directly related to the fluorescence lifetime of isolated CP29. For example, both Chls a603 and a616 are found at the interface between CP29 and CP47 [48], and thus likely regulate the flow of energy between the two complexes [47]. In addition, we recall that Chl a616 is likely lost during purification [47], and thus cannot contribute to the kinetics of isolated CP29. Therefore, we can imagine that the EET kinetics of isolated CP29 is somewhat different from the *in vivo* one. The strongest influence of Chls a603 and a616 on the PSII NPQ levels could be partially explained by the positions of these two Chls as energetic connections between the PSII core and the PSII antennas.

In the isolated solubilized CP29 complexes containing Vio, removal of Chl a612 caused the fastest fluorescence decay component to double its lifetime [56]. If this fastest component represents the fraction of quenched complexes in solution, these results show that the lifetime of quenched CP29 increases significantly upon removal of Chl a612. This effect is only reproduced by the Lutein model (Figure S12) in which Vio is removed. This seems to suggest that Vio has a limited participation to the quenching process. However, looking at the values of the couplings, we obtain that those between Vio and the closest Chls in site L2 have the same magnitude as the ones in site L1, as also seen in Ref. 28 (See Figure S1). A possible explanation of this apparent discrepancy could be related to the S_1 energy of Vio, which in CP29 might be significantly higher than the one of Lut.

LH-to-quenched conformational changes. Our results show a limited sensitivity of the quenching process to changes in the relative position of one Car-Chl pair. As a matter of fact, with the current parameters, the all-pigment EET model predicts that the quenching occurs independently of large variations in the Car-Chl couplings.

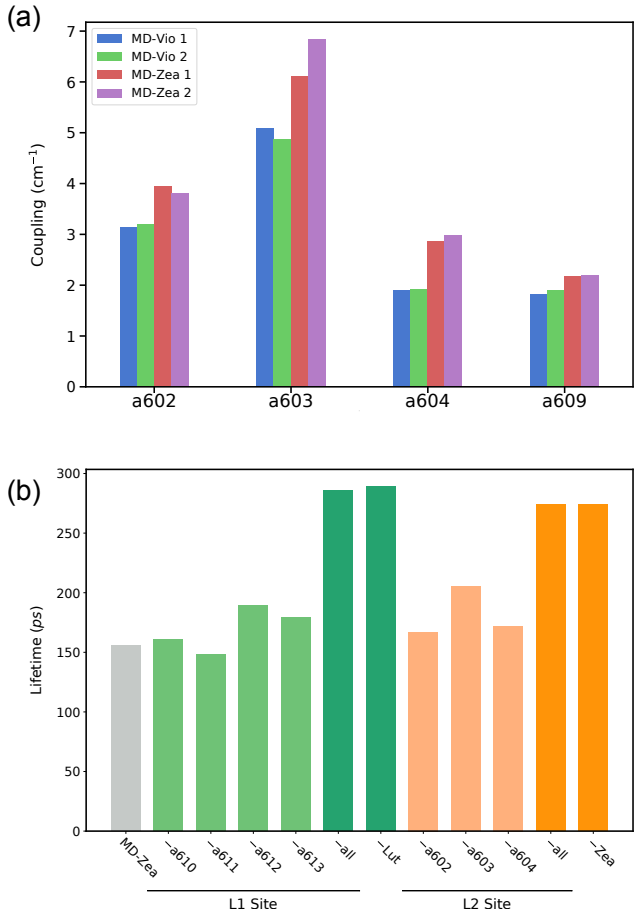

Figure 6: Effect of Zea on the quenching of CP29. (a) Comparison between Vio/Zea-Chls EET coupling values along MDs of CP29-Vio and CP29-Zea, respectively. The plot shows only the coupling values for the most significant Vio/Zea-Chls pairs of the Vio/Zea binding site. (b) Excited-state lifetime of CP29-Zea obtained by removing some of the couplings in the all-pigments Zea-model. Labels on the x-axis denote the couplings that have been set to zero. " - Lut" and " - Zea" denote kinetic models obtained by removing completely Lut or Zea.

A dramatic conformational change would thus be needed to reach a truly unquenched conformation. Even fully inactivating the L2(Vio/Zea) site as a possible quencher, is not sufficient to recover the lifetime of unquenched CP29. However, the model shows that a sharp switch between the quenched and unquenched lifetimes can be obtained by increasing the S_1 energy above 17 000 cm^{-1}. Of course, this energetic position is not an independent parameter, as it is tied to the spectral density of the S_1 state.

CP29-LHCII comparison. In the case of LHCII, both sites L1 and L2 are occupied by lutein [32, 65] but the two luteins are not equivalent: they have different conformations, according to the crystal structure [69], and different S_2 excitation energies [70]. More recently, it was shown that the L2 lutein also has a different electronic structure, and acts as an energy donor towards the Chls [71]. Finally, the S_1 energy of the L1 lutein in LHCII seems to be sensitive to the environment, and an increase in S_1-mediated energy dissipation was correlated to the energy of the S_1 state [72]. It was proposed that a change in the conformation of xanthophylls might cause an increase of EET coupling to the Chls, or more importantly a noticeable shift in their S_1 energy, allowing them to switch function, from energy donors to energy acceptors [62]. If this is the case, the quenching mechanism should be strongly dependent on the S_1 energy of Lut. Moreover, to be an efficient energy donor, the S_1 state of Cars should have a non-negligible coupling with Chls also in the unquenched conformation. This is in clear contrast with the notion of a S_1/Q_y coupling reduction in the unquenched state. In order to reconcile this apparent contrast, the quenching models will need to take into account the energetic modulation of the $S_1 \leftrightarrow Q_y$ EET direction.

5. Conclusions

The Chl(Q_y)-to-Car(S_1) EET model represents so far the most commonly used structure-based framework to understand NPQ in antenna complexes of plants. In this work we have presented a comprehensive analysis of the performance of this model when applied to CP29. To achieve a more complete and robust description we have combined the model with four independent 3 μs MD trajectories of CP29 embedding violaxanthin or zeaxanthin in the L2 site. We find that the model is rather insensitive to physically reasonable variations in single Chl-Car couplings when all pigments are involved in the network of interactions. A larger sensitivity is found when only considering the Lut/a612 pair but, also in this case, very large conformational changes would be required to modify the coupling and see the large change in the complex lifetime which characterizes the light-harvesting/quenching switch.

Our results, instead, show that a major role in regulating the quenching level is played by the Car S_1 energy, in line with very recent spectroscopy experiments.[56] The S_1 energy could be tuned by the Car conformation, by specific interactions with the protein, or simply by turning Vio into Zea. These findings call for a reassessment of the EET models of NPQ by explicitly considering how the Q_y/S_1 EET equilibrium is tuned by the Car properties.

Finally, we recall that some of us have recently proposed that quenching could proceed through charge-transfer states in trimeric LHCII [73]. The charge-transfer mechanism was predicted to be extremely selective and to occur only in the L1 site of LHCII, because both the electronic coupling and the driving force are sensitive to small variations in the Car-Chl distances and orientation and to different electric fields in the two sites. Taking into account also this mechanism could add a further explanation of how the antenna complexes switch to an unquenched state with a limited conformational change.

Declaration of competing interest

The authors declare that they have no known competing financial interests or personal relationships that could have appeared to influence the work reported in this paper.

Acknowledgments

L.C. and B.M. acknowledge funding by the European Research Council, under the grant ERC-AdG-786714 (LIFETimeS). M.L. acknowledges funding by University of Pisa under the grant BIHO. B.M. acknowledges financial support from MIUR through the PRIN 2017 (grant 201795SBA3_002).

Appendix A. Supplementary data

Supplementary data to this article can be found online at https://doi.org/10.1016/j.bbabio.XXXXX

References

[1] R. Croce, H. van Amerongen, Natural strategies for photosynthetic light harvesting, Nat. Chem. Bio. 10 (7) (2014) 492–501. doi:10.1038/nchembio.1555.

[2] P. Müller, X. P. Li, K. K. Niyogi, Non-photochemical quenching. A response to excess light energy., PLANT PHYSIOLOGY 125 (4) (2001) 1558–1566. doi:10.1104/pp.125.4.1558.

[3] N. E. Holt, G. R. Fleming, K. K. Niyogi, Toward an Understanding of the Mechanism of Nonphotochemical Quenching in Green Plants †, Biochemistry 43 (26) (2004) 8281–8289. doi:10.1021/bi0494020.

[4] A. V. Ruban, M. P. Johnson, C. D. Duffy, The photoprotective molecular switch in the photosystem II antenna., Biochim. Biophys. Acta - Bioenerg. 1817 (1) (2012) 167–181. doi:10.1016/j.bbabio.2011.04.007.

[5] A. V. Ruban, Light harvesting control in plants, FEBS Lett. 592 (2018) 3030–3039. doi:10.1002/1873-3468.13111.

[6] K. K. Niyogi, T. B. Truong, Evolution of flexible non-photochemical quenching mechanisms that regulate light harvesting in oxygenic photosynthesis, Current Opinion in Plant Biology 16 (3) (2013) 307–314.

[7] A. Pinnola, R. Bassi, Molecular mechanisms involved in plant photoprotection., Biochem. Soc. Trans. 46 (2) (2018) 467–482. doi:10.1042/bst20170307.

[8] D. I. Bennett, K. Amarnath, S. Park, C. J. Steen, J. M. Morris, G. R. Fleming, Models and mechanisms of the rapidly reversible regulation of photosynthetic light harvesting, Open Biol. 9 (4). doi:10.1098/rsob.190043.

[9] L. Nicol, W. J. Nawrocki, R. Croce, Disentangling the sites of non-photochemical quenching in vascular plants, Nat. Plantsdoi:10.1038/s41477-019-0526-5.

[10] L. Dall'Osto, S. Cazzaniga, M. Bressan, D. Paleček, K. Žídek, K. K. Niyogi, G. R. Fleming, D. Zigmantas, R. Bassi, Two mechanisms for dissipation of excess light in monomeric and trimeric light-harvesting complexes, Nature Plants 3 (5) (2017) 1–9.

[11] S. de Bianchi, N. Betterle, R. Kouril, S. Cazzaniga, E. Boekema, R. Bassi, L. Dall'Osto, Arabidopsis mutants deleted in the light-harvesting protein lhcb4 have a disrupted photosystem II macrostructure and are defective in photoprotection, Plant Cell 23 (7) (2011) 2659–2679. doi:10.1105/tpc.111.087320.

[12] Y. Miloslavina, S. de Bianchi, L. Dall'Osto, R. Bassi, A. R. Holzwarth, Quenching in arabidopsis thaliana mutants lacking monomeric antenna proteins of photosystem II, J. Biol. Chem. 286 (42) (2011) 36830–36840. doi:10.1074/jbc.m111.273227.

[13] A. A. Pascal, Z. Liu, K. Broess, B. Van Oort, H. Van Amerongen, C. Wang, P. Horton, B. Robert, W. Chang, A. Ruban, Molecular basis of photoprotection and control of photosynthetic light-harvesting, Nature 436 (7047) (2005) 134–137. doi:10.1038/nature03795.

[14] T. P. J. Krüger, E. Wientjes, R. Croce, R. van Grondelle, Conformational switching explains the intrinsic multifunctionality of plant light-harvesting complexes., Proceedings of the National Academy of Sciences of the United States of America 108 (33) (2011) 13516–13521.

[15] T. P. Krüger, C. Ilioaia, M. P. Johnson, A. V. Ruban, R. van Grondelle, Disentangling the low-energy states of the major light-harvesting complex of plants and their role in photoprotection, Biochim. Biophys. Acta - Bioenerg. 1837 (7) (2014) 1027–1038. doi:10.1016/j.bbabio.2014.02.014.

[16] L. Tian, E. Dinc, R. Croce, LHCII Populations in Different Quenching States Are Present in the Thylakoid Membranes in a Ratio that Depends on the Light Conditions, The Journal of Physical Chemistry Letters 6 (12) (2015) 2339–2344.

[17] T. Kondo, W. J. Chen, G. S. Schlau-Cohen, Single-molecule fluorescence spectroscopy of photosynthetic systems, Chem. Rev. 117 (2) (2017) 860–898. doi:10.1021/acs.chemrev.6b00195.

[18] X. P. Li, O. Björkman, C. Shih, A. R. Grossman, M. Rosenquist, S. Jansson, K. K. Niyogi, A pigment-binding protein essential for regulation of photosynthetic light harvesting., Nature 403 (6768) (2000) 391–395.

[19] X.-P. Li, P. Muller-Moule, A. M. Gilmore, K. K. Niyogi, PsbS-dependent enhancement of feedback de-excitation protects photosystem II from photoinhibition, Proceedings National Academy Sciences 99 (23) (2002) 15222–15227. doi:10.1073/pnas.232447699.

[20] J.-D. Rochaix, Regulation and Dynamics of the Light-Harvesting System, Annual Review of Plant Biology 65 (1) (2014) 287–309.

[21] A. V. Ruban, R. Berera, C. Ilioaia, I. H. M. van Stokkum, J. T. M. Kennis, A. A. Pascal, H. van Amerongen, B. Robert, P. Horton, R. van Grondelle, Identification of a mechanism of photoprotective energy dissipation in higher plants., Nature 450 (7169) (2007) 575–578.

[22] T. K. Ahn, T. J. Avenson, M. Ballottari, Y.-C. Cheng, K. K. Niyogi, R. Bassi, G. R. Fleming, Architecture of a Charge-Transfer State Regulating Light Harvesting in a Plant Antenna Protein, Science 320 (5877) (2008) 794–797. doi:10.1126/science.1154800.

[23] M. G. Müller, P. Lambrev, M. Reus, E. Wientjes, R. Croce, A. R. Holzwarth, Singlet energy dissipation in the photosystem II light-harvesting complex does not involve energy transfer to carotenoids, ChemPhysChem 11 (6) (2010) 1289–1296. doi:10.1002/cphc.200900852.

[24] S. Bode, C. C. Quentmeier, P.-N. Liao, N. Hafi, T. Barros, L. Wilk, F. Bittner, P. J. Walla, On the regulation of photosynthesis by excitonic interactions between carotenoids and chlorophylls, Proc. Natl. Acad. Sci. 106 (30) (2009) 12311–12316. doi:10.1073/pnas.0903536106.

[25] C. D. P. Duffy, J. Chmeliov, M. Macernis, J. Sulskus, L. Valkunas, a. V. Ruban, Modeling of Fluorescence Quenching by Lutein in the Plant Light-Harvesting Complex LHCII, J. Phys. Chem. B 117 (38) (2013) 10974–10986. doi:10.1021/jp3110997.

[26] J. Chmeliov, W. P. Bricker, C. Lo, E. Jouin, L. Valkunas, A. V. Ruban, C. D. Duffy, An 'all pigment' model of excitation quenching in LHCII, Phys. Chem. Chem. Phys. 17 (24) (2015) 15857–15867. doi:10.1039/c5cp01905b.

[27] K. F. Fox, V. Balevičius, J. Chmeliov, L. Valkunas, A. V. Ruban, C. D. Duffy, The carotenoid pathway: What is important for excitation quenching in plant antenna complexes?, Phys. Chem. Chem. Phys. 19 (34) (2017) 22957–22968. doi:10.1039/c7cp03535g.

[28] K. F. Fox, C. Ünlü, V. Balevičius, B. N. Ramdour, C. Kern, X. Pan, M. Li, H. van Amerongen, C. D. Duffy, A possible molecular basis for photoprotection in the minor antenna proteins of plants, Biochim. Biophys. Acta - Bioenerg. 1859 (7)

(2018) 471–481. doi:10.1016/j.bbabio.2018.03.015.
[29] V. Balevičius, K. F. Fox, W. P. Bricker, S. Jurinovich, I. G. Prandi, B. Mennucci, C. D. P. Duffy, Fine control of chlorophyll-carotenoid interactions defines the functionality of light-harvesting proteins in plants, Sci. Rep. 7 (1) (2017) 13956. doi:10.1038/s41598-017-13720-6.
[30] V. Daskalakis, S. Maity, C. L. Hart, T. Stergiannakos, C. D. P. Duffy, U. Kleinekathöfer, Structural Basis for Allosteric Regulation in the Major Antenna Trimer of Photosystem II, J. Phys. Chem. B 123 (45) (2019) 9609–9615. doi:10.1021/acs.jpcb.9b09767.
[31] X. Pan, M. Li, T. Wan, L. Wang, C. Jia, Z. Hou, X. Zhao, J. Zhang, W. Chang, Structural insights into energy regulation of light-harvesting complex CP29 from spinach., Nat. Struct. Mol. Biol. 18 (3) (2011) 309–15. doi:10.1038/nsmb.2008.
[32] X. Pan, Z. Liu, M. Li, W. Chang, Architecture and function of plant light-harvesting complexes II., Curr. Opin. Struct. Biol. 23 (4) (2013) 515–25. doi:10.1016/j.sbi.2013.04.004.
[33] X. Wei, X. Su, P. Cao, X. Liu, W. Chang, M. Li, X. Zhang, Z. Liu, Structure of spinach photosystem II–LHCII supercomplex at 3.2–AA resolution, Nature 534 (7605) (2016) 69–74. doi:10.1038/nature18020.
[34] B. Demmig, K. Winter, A. Krüger, F.-C. Czygan, Photoinhibition and zeaxanthin formation in intact leaves, Plant Physiology 84 (2) (1987) 218–224. doi:10.1104/pp.84.2.218.
[35] P. Jahns, D. Latowski, K. Strzalka, Mechanism and regulation of the violaxanthin cycle: The role of antenna proteins and membrane lipids, Biochim. Biophys. Acta (BBA) - Bioenergetics 1787 (1) (2009) 3–14. doi:10.1016/j.bbabio.2008.09.013.
[36] H. A. Frank, A. Cua, V. Chynwat, A. Young, D. Gosztola, M. R. Wasielewski, Photophysics of the carotenoids associated with the xanthophyll cycle in photosynthesis, Photosynth. Res. 41 (3) (1994) 389–395. doi:10.1007/bf02183041.
[37] P. Xu, L. Tian, M. Kloz, R. Croce, Molecular insights into zeaxanthin-dependent quenching in higher plants, Sci. Rep. 5 (1) (2015) 13679. doi:10.1038/srep13679.
[38] K. K. Niyogi, A. R. Grossman, O. Björkman, Arabidopsis mutants define a central role for the xanthophyll cycle in the regulation of photosynthetic energy conversion, Plant Cell 10 (7) (1998) 1121–1134. doi:10.1105/tpc.10.7.1121.
[39] L. Cupellini, S. Jurinovich, I. G. Prandi, S. Caprasecca, B. Mennucci, Photoprotection and triplet energy transfer in higher plants: The role of electronic and nuclear fluctuations, Physical Chemistry Chemical Physics 18 (16) (2016) 11288–11296. doi:10.1039/c6cp01437b.
[40] K. Ogata, T. Yuki, M. Hatakeyama, W. Uchida, S. Nakamura, All-atom molecular dynamics simulation of photosystem II embedded in thylakoid membrane, Journal of the American Chemical Society 135 (42) (2013) 15670–15673. doi:10.1021/ja404317d.
[41] J. A. Maier, C. Martinez, K. Kasavajhala, L. Wickstrom, K. E. Hauser, C. Simmerling, ff14SB: Improving the Accuracy of Protein Side Chain and Backbone Parameters from ff99SB, Journal of Chemical Theory and Computation 11 (8) (2015) 3696–3713. doi:10.1021/acs.jctc.5b00255.
[42] C. J. Dickson, B. D. Madej, Å. A. Skjevik, R. M. Betz, K. Teigen, I. R. Gould, R. C. Walker, Lipid14: The amber lipid force field, Journal of Chemical Theory and Computation 10 (2) (2014) 865–879. doi:10.1021/ct4010307.
[43] L. Zhang, D. A. Silva, Y. Yan, X. Huang, Force field development for cofactors in the photosystem II, Journal of Computational Chemistry 33 (25) (2012) 1969–1980. doi:10.1002/jcc.23016.
[44] I. G. Prandi, L. Viani, O. Andreussi, B. Mennucci, Combining classical molecular dynamics and quantum mechanical methods for the description of electronic excitations: The case of carotenoids, Journal of Computational Chemistry 37 (11) (2016) 981–991. doi:10.1002/jcc.24286.
[45] D. A. Case, Amber 18, University of California, San Francisco.
[46] D. R. Roe, T. E. Cheatham, PTRAJ and CPPTRAJ: Software for processing and analysis of molecular dynamics trajectory data, J. Chem. Theory Comput. 9 (7) (2013) 3084–3095. doi:10.1021/ct400341p.
[47] P. Xu, L. M. Roy, R. Croce, Functional organization of photosystem II antenna complexes: CP29 under the spotlight, Biochim. Biophys. Acta - Bioenerg. 1858 (10) (2017) 815–822. doi:10.1016/j.bbabio.2017.07.003.
[48] L. S. van Bezouwen, S. Caffarri, R. S. Kale, R. Kouřil, A.-M. W. H. Thunnissen, G. T. Oostergetel, E. J. Boekema, Subunit and chlorophyll organization of the plant photosystem II supercomplex, Nat. Plants 3 (7) (2017) 17080. doi:10.1038/nplants.2017.80.
[49] T. Renger, R. A. Marcus, On the relation of protein dynamics and exciton relaxation in pigment-protein complexes: An estimation of the spectral density and a theory for the calculation of optical spectra, J. Chem. Phys. 116 (22) (2002) 9997–10019. doi:10.1063/1.1470200.
[50] P. J. Walla, P. A. Linden, K. Ohta, G. R. Fleming, Excited-State Kinetics of the Carotenoid S 1 State in LHC II and Two-Photon Excitation Spectra of Lutein and β-Carotene in Solution: Efficient Car S 1 $\rightarrow$ Chl Electronic Energy Transfer via Hot S_1 States? , J. Phys. Chem. A 106 (10) (2002) 1909–1916. doi:10.1021/jp011495x.
[51] F. Müh, D. Lindorfer, M. Schmidt am Busch, T. Renger, Towards a structure-based exciton Hamiltonian for the CP29 antenna of photosystem II., Phys. Chem. Chem. Phys. 16 (24) (2014) 11848–63. doi:10.1039/c3cp55166k.
[52] T. Polívka, V. Sundström, Ultrafast dynamics of carotenoid excited States-from solution to natural and artificial systems., Chem. Rev. 104 (4) (2004) 2021–71. doi:10.1021/cr020674n.
[53] M. E. Madjet, A. Abdurahman, T. Renger, Intermolecular coulomb couplings from ab initio electrostatic potentials: Application to optical transitions of strongly coupled pigments in photosynthetic antennae and reaction centers, J. Phys. Chem. B 110 (34) (2006) 17268–17281. doi:10.1021/jp0615398.
[54] O. Andreussi, S. Knecht, C. M. Marian, J. Kongsted, B. Mennucci, Carotenoids and light-harvesting: from DFT/MRCI to the Tamm-Dancoff approximation, J. Chem. Theory Comput. (2015) 150115132521009doi:10.1021/ct5011246.
[55] D. Khokhlov, A. Belov, Ab initio model for the chlorophyll-lutein exciton coupling in the LHCII complex, Biophys. Chem. 246 (January) (2019) 16–24. doi:10.1016/j.bpc.2019.01.001.
[56] V. Mascoli, N. Liguori, P. Xu, L. M. Roy, I. H. van Stokkum, R. Croce, Capturing the Quenching Mechanism of Light-Harvesting Complexes of Plants by Zooming in on the Ensemble, Chem 5 (11) (2019) 2900–2912. doi:10.1016/j.chempr.2019.08.002.
[57] M. H. Shabestari, C. J. Wolfs, R. B. Spruijt, H. van Amerongen, M. Huber, Exploring the structure of the 100 amino-acid residue long n-terminus of the plant antenna protein CP29, Biophys. J. 106 (6) (2014) 1349–1358. doi:10.1016/j.bpj.2013.11.4506.
[58] N. Liguori, X. Periole, S. J. Marrink, R. Croce, From light-harvesting to photoprotection: structural basis of the dynamic switch of the major antenna complex of plants (LHCII), Sci. Rep. 5 (October) (2015) 15661. doi:10.1038/srep15661.
[59] P. López-Tarifa, N. Liguori, N. van den Heuvel, R. Croce, L. Visscher, Coulomb couplings in solubilised light harvesting complex II (LHCII): challenging the ideal dipole approximation from TDDFT calculations, Phys. Chem. Chem. Phys. 19 (28) (2017) 18311–18320. doi:10.1039/c7cp03284f.
[60] P. Horton, A. V. Ruban, M. Wentworth, Allosteric regulation of the light-harvesting system of photosystem II, Philos. Trans. R. Soc. B Biol. Sci. 355 (1402) (2000) 1361–1370. doi:10.1098/rstb.2000.0698.
[61] M. Tutkus, F. Saccon, J. Chmeliov, O. Venckus, I. Ciplys, A. V. Ruban, L. Valkunas, Single-molecule microscopy studies of LHCII enriched in Vio or Zea., Biochim. Biophys. Acta - Bioenerg. 1860 (December 2018) (2019) 0–1. doi:10.1016/j.bbabio.2019.05.002.
[62] N. Liguori, P. Xu, I. H. Van Stokkum, B. Van Oort, Y. Lu, D. Karcher, R. Bock, R. Croce, Different carotenoid conformations have distinct functions in light-harvesting regulation in

plants, Nat. Commun. 8 (1) (2017) 1–9. doi:10.1038/s41467-017-02239-z.

[63] T. Polívka, V. Sundström, Dark excited states of carotenoids: Consensus and controversy, Chem. Phys. Lett. 477 (1-3) (2009) 1–11. doi:10.1016/j.cplett.2009.06.011.

[64] S. Maity, A. Gelessus, V. Daskalakis, U. Kleinekathöfer, On a chlorophyll-caroteinoid coupling in LHCII, Chem. Phys. 526 (May) (2019) 110439. doi:10.1016/j.chemphys.2019.110439.

[65] Z. Liu, H. Yan, K. Wang, T. Kuang, J. Zhang, L. Gui, X. An, W. Chang, Crystal structure of spinach major light-harvesting complex at 2.72 Å resolution, Nature 428 (6980) (2004) 287–292. doi:10.1038/nature02373.

[66] M. Son, A. Pinnola, S. C. Gordon, R. Bassi, G. S. Schlau-Cohen, Observation of dissipative chlorophyll-to-carotenoid energy transfer in light-harvesting complex II in membrane nanodiscs, Nat. Commun. 11 (1). doi:10.1038/s41467-020-15074-6.

[67] D. A. Gacek, C.-P. Holleboom, P.-N. Liao, M. Negretti, R. Croce, P. J. Walla, Carotenoid dark state to chlorophyll energy transfer in isolated light-harvesting complexes CP24 and CP29, Photosynth. Res. 143 (1) (2020) 19–30. doi:10.1007/s11120-019-00676-z.

[68] Z. Guardini, M. Bressan, R. Caferri, R. Bassi, L. Dall'Osto, Identification of a pigment cluster catalysing fast photoprotective quenching response in CP29, Nat. Plants 6 (3) (2020) 303–313. doi:10.1038/s41477-020-0612-8.

[69] H. Yan, P. Zhang, C. Wang, Z. Liu, W. Chang, Two lutein molecules in LHCII have different conformations and functions: Insights into the molecular mechanism of thermal dissipation in plants, Biochem. Biophys. Res. Commun. 355 (2) (2007) 457–463. doi:10.1016/j.bbrc.2007.01.172.

[70] M. M. Mendes-Pinto, D. Galzerano, A. Telfer, A. A. Pascal, B. Robert, C. Ilioaia, Mechanisms Underlying Carotenoid Absorption in Oxygenic Photosynthetic Proteins, J. Biol. Chem. 288 (26) (2013) 18758–18765. doi:10.1074/jbc.M112.423681.

[71] M. Son, A. Pinnola, R. Bassi, G. S. Schlau-Cohen, The Electronic Structure of Lutein 2 Is Optimized for Light Harvesting in Plants, Chem 5 (3) (2019) 575–584. doi:10.1016/j.chempr.2018.12.016.

[72] M. Son, A. Pinnola, G. S. Schlau-Cohen, Zeaxanthin independence of photophysics in light-harvesting complex II in a membrane environment, Biochim. Biophys. Acta - Bioenerg. 1861 (5-6) (2020) 148115. doi:10.1016/j.bbabio.2019.148115.

[73] L. Cupellini, D. Calvani, D. Jacquemin, B. Mennucci, Charge transfer from the carotenoid can quench chlorophyll excitation in antenna complexes of plants, Nat. Commun. 11 (1) (2020) 662. doi:10.1038/s41467-020-14488-6.